

Chemical Characterization of BiFeO₃ Obtained by Pechini Method

Elídia A. Vetter Ferri,^a Ivair A. Santos,^b Eduardo Radovanovic,^a
Rafaelle Bonzanini^c and Emerson Marcelo Giroto^{*a}

^a Departamento de Química, Universidade Estadual de Maringá, Av. Colombo 5790, 87020-900 Maringá-PR, Brazil

^b Departamento de Física, Universidade Estadual de Maringá, Av. Colombo 5790, 87020-900, Maringá-PR, Brazil

^c Instituto de Química, Universidade Estadual de Campinas, CP 6154, 13083-970 Campinas-SP, Brazil

Este trabalho descreve a síntese e a caracterização de BiFeO₃ obtido a partir da rota Pechini, utilizando-se nitrato de bismuto e nitrato de ferro como precursores. Os pós foram calcinados a 800 °C em ar durante 2 h. Os difratogramas de raios X mostraram que o material apresenta duas fases, BiFeO₃ (95%) e α-Bi₂O₃ (5%). A transição de fase ferroelétrica da amostra em 821 °C foi detectada por análise térmica diferencial. Os resultados das análises por microscopia eletrônica de varredura (SEM), espectroscopia de energia dispersiva (EDS) e fluorescência de raios X por dispersão de energia (EDX) mostraram que a amostra é quimicamente homogênea. As imagens de microscopia eletrônica de transmissão revelaram que a amostra é uniforme e apresenta partículas com formato esférico e tamanho médio de 30 nm.

This work describes the synthesis and characterization of BiFeO₃ obtained by the Pechini route using bismuth nitrate and iron nitrate as precursors. The powders were annealed at 800 °C in air for 2 h. X-ray diffraction patterns showed that the material presents two phases, BiFeO₃ (95%) and α-Bi₂O₃ (5%). The ferroelectric transition of the sample at 821 °C was detected by differential thermal analysis. Results of analyses by scanning electron microscopy (SEM), energy dispersive spectroscopy (EDS) and energy dispersive X-ray fluorescence (EDX) showed that the sample is chemically homogeneous. Transmission electron microscopy images revealed that the sample is uniform and contains spherical particles with an average size of 30 nm.

Keywords: Pechini method, X-ray diffraction, ferroelectricity, magnetic properties

Introduction

Multiferroic magnetoelectric materials are known to exhibit magnetic (ferro, anti, or ferri) and electric (ferro) ordering simultaneously at room temperature,¹ as well as interesting physical properties with possible practical applications, as in new memory devices whose polarization and magnetization states and coupling can be simultaneously exploited.²⁻⁶ BiFeO₃ is one of these few materials, along with YMnO₃ and BiMnO₃, that have all the potential applications of both their parent ferroelectric and ferromagnetic materials.

Bismuth ferrite, BiFeO₃, belongs to the perovskite class of materials with a rhombohedrally distorted unit cell. It has the polar *R3c* space group, whose ions are displaced along the [111] direction relative to the ideal centrosymmetric

positions.^{7,8} Detailed structural investigations of BiFeO₃ can be found elsewhere.^{9,10} The interest in this compound is due to its ferroelectric behavior with a high Curie temperature (*T_C* ca. 1100 K) and its antiferromagnetic behavior with a relatively high Néel temperature (*T_N* ca. 650 K).^{7,11} Both BiFeO₃ thin films and ceramics have been intensively investigated in the last years.¹¹⁻¹⁹

Multiferroic BiFeO₃ was discovered in the 1960s and its properties have been extensively studied. However, the electrical properties of pure BiFeO₃ have rarely been reported on and it has no commercial applications due to its room-temperature low resistivity, which may originate from uncertain oxygen stoichiometry, high defect density, and poor sample quality. This low resistivity hinders the movement of the ferroelectric domains under applied electric field and prevents the ferroelectric hysteretic behavior, which is fundamental for practical applications in memory devices and others.

*e-mail: emgirotto@uem.br

In order to understand the properties of BiFeO₃, it is very important to establish a synthesis procedure in a manner such as to avoid impurity phases. There are several reports on the synthesis of BiFeO₃. Recently, BiFeO₃ ceramic samples have been synthesized by methods like pulsed laser deposition,¹² sol-gel,¹²⁻¹³ solid state reaction,¹⁴ simple precipitation,¹⁵ rapid liquid phase sintering,¹⁶ chemical solution deposition¹⁷ and high-energy ball milling.¹⁸

For electronic materials and other applications such as optics, catalysis and thermomechanics, the precise control of the manufacturing process is always crucial, because many physical properties depend on the manufacturing process closely.¹⁹ In this context, it becomes apparent that the traditional solid state reaction processes do not ensure either high compositional homogeneity or suitable purity, or allow a morphological or microstructural control. In contrast, low-temperature manufacture methods referred to as “soft chemistry”, such as the Pechini method, produce more homogeneous, purer, and more reproducible phases whose microstructure and morphology may be controlled practically at will.^{19,20} These aspects play a major role in determining the overall electronic, optical, magnetic and catalytic properties, as well as the applicability of multiple-oxide materials. Besides saving energy and being cost effective, the Pechini method is a versatile process that allows the simple and quick preparation of ceramic materials.²¹

In the present research, BiFeO₃ powders were synthesized by the Pechini method using nitrates as precursors and citric acid as a chelating agent. The samples were characterized by X-ray diffractometry, thermal analysis, EDS, EDX, FTIR and transmission electron microscopy. Besides obtaining a 95% pure multiferroic material through the Pechini method, the main goal of this work was to identify the chemical aspects that affect its stoichiometry and thus its physical properties.

Experimental

Synthesis of BiFeO₃

All reagents were of analytical grade and were used without further purification or treatment. Deionized water was used in the preparation of all samples. Bismuth ferrite was prepared by thermal decomposition of polymeric mixed-metal precursor gels. The polymeric precursor solution was prepared by the Pechini method.²¹ The process was based on metal citrate polymerization with ethylene glycol. A hydrocarboxylic acid, such as citric

acid, was added to the aqueous solution to chelate cations. The addition of a polyalcohol, such as ethylene glycol, led to the formation of an organic ester. Polymerization was promoted by heating and resulted in a homogeneous resin with metal ions uniformly distributed throughout the organic matrix. The sols were prepared by dissolving citric acid in deionized water with constant stirring and kept at 60-70 °C. Then, bismuth nitrate [Bi(NO₃)₃·5H₂O] (98%) (Aldrich) and ferric nitrate [Fe(NO₃)₃·9H₂O] (> 99%) (Aldrich), 1:1 molar ratio, were added to the mixture. After their total dissolution, citric acid/ethylene glycol (Synth) was added at 60:40 mass ratio. The temperature was raised up to 90-110 °C to promote esterification. The orange gel formed at the end of the reaction was dried overnight at 100 °C to remove excess water. The gel was heat-treated at 800 °C in air for 2 h to form the oxide. During the annealing procedure, the furnace heating and cooling rates were kept at 10 °C min⁻¹ and 20 °C min⁻¹ (accuracy of ± 1 °C), respectively.

X-ray diffraction analysis

Powder X-ray diffraction (XRD) measurements were carried out with a Shimadzu XD-3A, model VG-108R apparatus with Cu K_α radiation. The profile was refined using FullProf Suite software²² and the hexagonal unit cell corresponded to the R3c space group.

FTIR analysis

The FTIR spectra of the samples (prepared as KBr pellets) were recorded on a Bomem spectrophotometer, model MB-100. Thermogravimetric and differential thermal analyses were carried out on a SDTQ600 TA Instruments apparatus from room temperature to 1000 °C at 10 °C min⁻¹ in synthetic air.

TEM and SEM analyses

Transmission electron micrographs were obtained with a 120 kV JEOL instrument. The samples were suspended in water and allowed to settle for 15 min. Then, a drop of the supernatant dispersion was placed onto a carbon film supported by a copper grid. Bi, Fe, and O mapping and quantities were checked by energy dispersive spectroscopy analysis (EDS) and energy dispersive micro X-ray fluorescence analysis (EDX). The equipment used was an EDS Noran System Six (model 6714A-1SUS-SN, Thermo Electron Corp.) coupled to a Jeol JSM 6360-LV scanning electron microscope and an EDX spectrometer, Shimadzu, μEDX-1300.

Results and Discussion

The X-ray diffraction pattern suggests the formation of highly crystalline BiFeO_3 ($R3c$ space group), Figure 1. Most of the powder (95%, determined by Rietveld refinement, R factors: $R_p = 14.0$, $R_{wp} = 19.1$, $R_{exp} = 9.35$, $R_b = 18.7$) was the rhombohedrally distorted perovskite BiFeO_3 , with lattice parameters $a = b = 5.5832 \text{ \AA}$ and $c = 13.8804 \text{ \AA}$. The XRD patterns are in excellent accord with the JCPDS Card No. 14-0181 powder data. In addition, the formation of a spurious phase $\alpha\text{-Bi}_2\text{O}_3$ (5%) was evidenced, which may contribute to degrade the ferroelectric response of ceramics and thin films composed of the $\text{BiFeO}_3 + \text{Bi}_2\text{O}_3$ mixture, whereas the electrical conductivity of devices containing this mixture will certainly be higher than that of pure BiFeO_3 . However, the magnetic properties of the material are not intensely affected. In this way, in electro-electronic devices (prototypal thin films in random access memories, for example) in which $\text{BiFeO}_3 + \text{Bi}_2\text{O}_3$ is submitted to magnetic fields, their performance will hardly be affected.

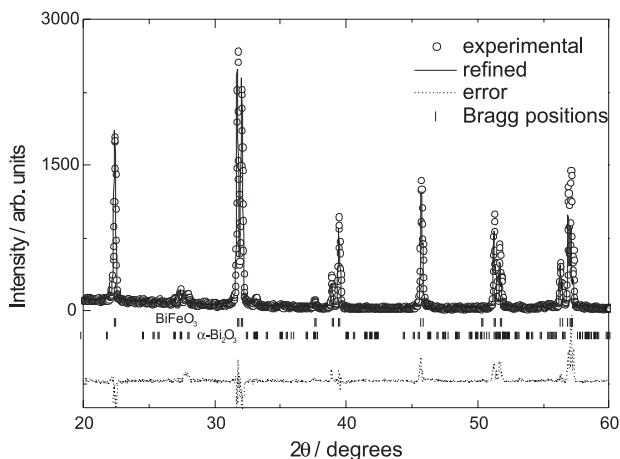


Figure 1. XRD patterns and Rietveld refinement of BiFeO_3 powder annealed at $800 \text{ }^\circ\text{C}$.

The infrared spectrum (Figure 2) shows a curvature from 1000 to 4000 cm^{-1} , which is characteristic of semiconductors.²³ The bands at around 3400 cm^{-1} and 1600 cm^{-1} are assigned to water absorbed after calcination. The strong peak at *ca.* 550 cm^{-1} may be assigned to Fe-O interaction.²⁴

TGA-DTA experiments (Figure 3) were used to investigate thermal degradation and phase transition characteristics. The small endothermic peak in the DTA trace at *ca.* $821 \text{ }^\circ\text{C}$ has been assigned to ferroelectric-to-paraelectric phase transition. It must be mentioned that there is no agreement on the value of the Curie point of bismuth ferrite processed by different methods, *i.e.*, 823 ,¹⁷

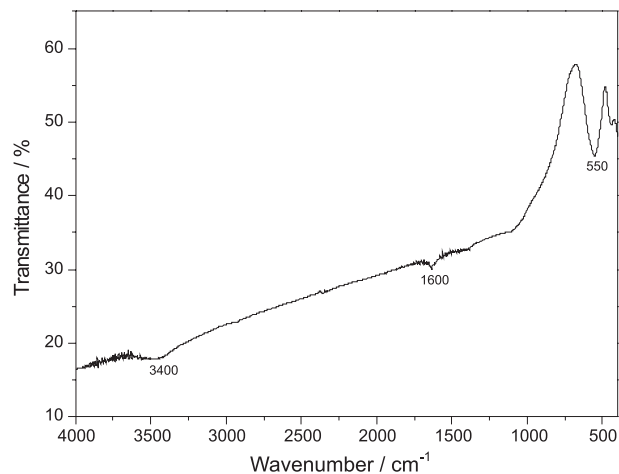


Figure 2. FTIR spectrum of BiFeO_3 powder.

821 ,⁶ 830.9 ,²⁵ and $836 \text{ }^\circ\text{C}$.²⁶ It seems that the Curie transition temperature of bismuth ferrite may vary slightly depending on sample processing conditions and the synthesis methods. As the melting point of Bi_2O_3 is $817\text{-}825 \text{ }^\circ\text{C}$, this transition may also be assigned to the melting of this compound.¹⁴ TGA analysis showed 0.2% of weight loss up to *ca.* $650 \text{ }^\circ\text{C}$, probably due to the loss of residual compounds after calcination, probably trapped nitrates²⁷ (also confirmed from FTIR traces in the $1340\text{-}1440 \text{ cm}^{-1}$ range, Figure 2). The weight loss above $805 \text{ }^\circ\text{C}$ may be assigned to the sublimation of residual Bi_2O_3 .¹⁴

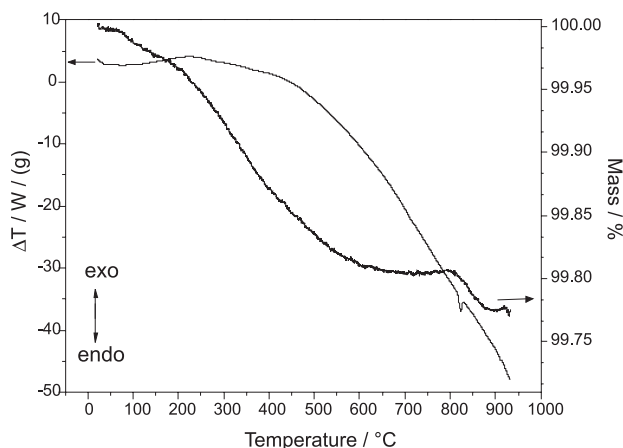


Figure 3. TGA and DTA (heating) curves of BiFeO_3 powder.

Figure 4a shows the distribution of Bi, Fe, and O within an agglomerate of nanoparticles. It was possible to verify that Bi, Fe (Figure 4b), and O are well distributed in the sample. Energy dispersive X-ray fluorescence (EDX) analysis disregarding O and C indicated 82% of Bi and 18% of Fe in atomic percentage. These percentages show that the sample is almost chemically homogeneous (regarding Bi:Fe = 1:1) with a Bi/Fe atomic percent ratio equal to

1.1. This ratio means that *ca.* 10% excess Bi is present (or Fe is lacking). In fact, the residual α -Bi₂O₃ identified through XRD analysis can be explained considering this stoichiometric deviation. Considering that iron nitrate is hygroscopic, a fraction of the precursor could contain more water molecules than indicated in the flask label. In fact, its thermogravimetric analysis (not shown) revealed 10.84 H₂O molecules per Fe(NO₃)₃ unit. Thus, iron nitrate used in the synthesis had more water than presumed; in other words, the weighed mass had a lower amount of iron than thought. Although this conclusion may sound common place, an exam of the literature shows that no explanations for the existence of impurities and/or unexpected phases in Pechini synthesis had been offered yet. However, we have grounds to propose that unexpected amounts of water in the precursors are a possible cause of impurities and/or unexpected phases in multiple oxide materials. Furthermore, this finding also evidences the key role of fine synthesis precursor stoichiometry in Pechini method, an aspect so far disregarded. In addition to the stoichiometry, it is necessary to mention that parameters such as calcination temperature, non-ideal calcination atmosphere, and precursor and solvent purity require some attention as well. We are currently investigating these parameters to optimize the BiFeO₃ synthesis. These results will be published shortly.

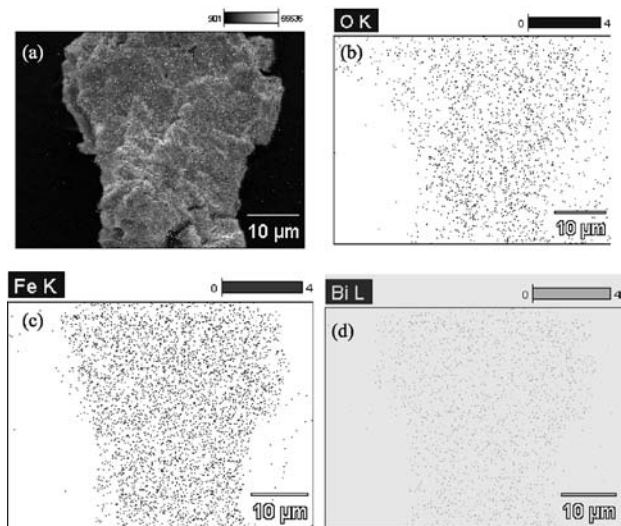


Figure 4. (a) Microparticle micrograph. (b), (c), and (d) are O(K), Fe(K), and Bi(L) EDS mappings, respectively.

Figure 5 displays a TEM image of the BiFeO₃ sample. Since the particles are superimposed onto an agglomerate core, the boundary limit of each nanoparticle is diffuse. Thus, it is not possible to measure the size of each individual particle accurately. However, particles with a mean size

of *ca.* 30 nm in diameter with a grain size distribution centered at 32 nm (normal distribution shown in the inset) and with low dispersion may be seen in the TEM images. Although the Pechini route is one of the most widely used methods to prepare ceramics with improved properties comparatively to those of ceramics prepared through conventional procedures,^{28,29} nanosized powder preparation control has not been achieved yet. Thus, the preparation of the nanosized particles by the Pechini method achieved in this work is an extra advantage over traditional solid state routes.

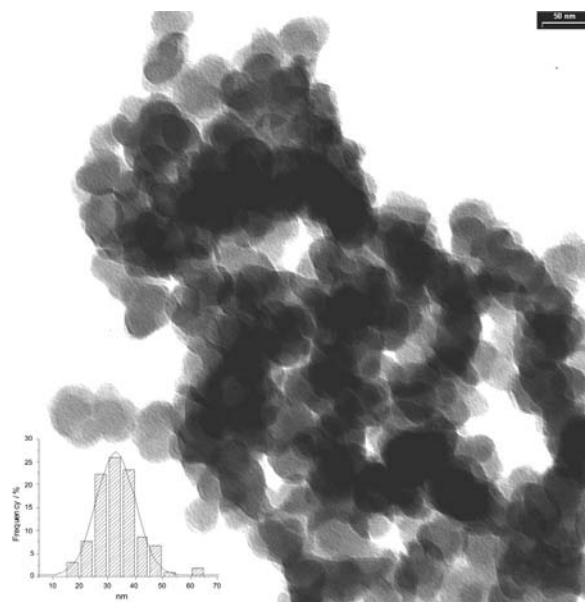


Figure 5. TEM image of nanocrystalline BiFeO₃ calcined at 800 °C. Inset: normal distribution of particle sizes.

Conclusions

The synthesis of BiFeO₃ through the Pechini method resulted in the formation of a highly crystalline BiFeO₃ perovskite, homogeneously distributed and with a low grain size. An unexpected phase (5% of Bi₂O₃) was identified and attributed mainly to pre-calcination precursor stoichiometry. DTA analysis indicates a ferroelectric phase transition temperature of 821 °C.

Acknowledgments

The authors thank Fundação Araucária (protocols 8772 and 7437) and CNPq (processes 470862/2006-8 and 556542/2005-3) for financial support, as well as UNICAMP for XRD measurements and Prof. M. C. Gonçalves for TEM images. E. V. F. and R. B. thank CAPES and CNPq for fellowships.

References

1. Hill, N. A.; *J. Phys. Chem. B* **2000**, *104*, 6694.
2. Kim, J. K.; Kim, S. S.; Kim, W.-J.; *Mater. Lett.* **2005**, *59*, 4006.
3. Zhu, W. M.; Ye, Z.-G.; *Ceram. Int.* **2004**, *30*, 1435.
4. Hur, N.; Park, S.; Sharma, P. A.; Ahn, J. S.; Guha, S.; Cheong, S.-W.; *Nature* **2004**, *429*, 392.
5. Kimura, T.; Kawamoto, S.; Yamada, I.; Azuma, M.; Takano, M.; Tokura, Y.; *Phys. Rev. B* **2003**, *67*, 180401.
6. Dho, J.; Leung, C. W.; MacManus-Driscoll, J. L.; Blamire, M. G.; *J. Cryst. Growth* **2004**, *267*, 548.
7. Ederer, C.; Spaldin, N. A.; *Phys. Rev. B* **2005**, *71*, 224103.
8. Li, Y. W.; Sun, J. L.; Chen, J.; Meng, X. J.; Chu, J. H.; *J. Cryst. Growth* **2005**, *285*, 595.
9. Kubel, F.; Schmid, H.; *J. Cryst. Growth* **1993**, *129*, 515.
10. Kubel, F.; Schmid, H.; *Acta Cryst. Sect. B: Struct. Sci.* **1990**, *46*, 698.
11. Wang, Y.; Jiang, Q.-h.; He, H.-c.; Nan, C.-W.; *Appl. Phys. Lett.* **2006**, *88*, 142503.
12. Gosh, S.; Dasgupta, S.; Sen, A.; Maiti, H. S.; *Mater. Res. Bull.* **2005**, *40*, 2073.
13. Liu, H.; Liu, Z.; Liu, Q.; Yao, K.; *Thin Solid Films* **2005**, *500*, 105.
14. Pradhan, A. K.; Zang, K.; Hunter, D.; Dadson, J. B.; Loutts, G. B.; Bhattacharya, P.; Katiyar, R.; Zhang, J.; Sellmyer, D. J.; Roy, U. N.; Cui, Y.; Burger, A.; *J. Appl. Phys.* **2005**, *97*, 093903.
15. Thapa, D.; Palkar, V. R.; Kurup, M. B.; Malik, S. K.; *Mater. Lett.* **2004**, *58*, 2692.
16. Wang, Y. P.; Zhou, L.; Zhang, M. F.; Chen, X. Y.; Liu, J. -M.; Liu, Z. G.; *Appl. Phys. Lett.* **2004**, *84*, 1731.
17. Iakovlev, S.; Solterbeck, C.-H.; Kuhnke, M.; Es-Souni, M.; *J. Appl. Phys.* **2005**, *97*, 094901.
18. Santos, I. A.; Grande, H. L. C.; Freitas, V. F.; de Medeiros, S. N.; Paesano Jr., A.; Cótica, L. F.; Radovanovic, E.; *J. Non-Cryst. Solids* **2006**, *352*, 3721.
19. Rousset, A.; *Solid State Ionics* **1996**, *84*, 293.
20. Fernández, J. D. G.; Melo, D. M. A.; Zinner, L. B.; Salustiano, C. M.; Silva, Z. R.; Martinelli, A. E.; Cerqueira, M.; Júnior, C. A.; Longo, E.; Bernardi, M. I. B.; *Mater. Lett.* **2002**, *53*, 122.
21. Pechini, M. P.; *U.S. pat. 3,330,697* **1967**.
22. Rodríguez-Carvajal, J.; *Phys. B* **1993**, *192*, 55.
23. Nakamoto, K.; *Infrared and Raman Spectra of Inorganic and Coordination Compounds*. 5th ed., Wiley: New York, 1997.
24. Sócrates, G.; *Infrared and Raman Characteristic Group Frequencies*. 3rd ed., Wiley: New York, 2001.
25. Wang, Y. P.; Yuan, G. L.; Chen, X. Y.; Liu, J. -M.; Liu, Z. G.; *J. Phys. D: Appl. Phys.* **2006**, *39*, 2019.
26. Kumar, M. M.; Palkar, V. R.; Srinivas, K.; Suryanarayana, S.; *Appl. Phys. Lett.* **2004**, *76*, 2764.
27. Nakagawa, I.; Walter, J. L.; *J. Chem. Phys.* **1969**, *51*, 1389.
28. Kahoul, A.; Nkeng, P.; Hammouche, A.; Nâamoune, F.; Poillerat, G.; *J. Solid State Chem.* **2001**, *161*, 379.
29. Xu, Y. B.; Yuan, X.; Huang, G. H.; Long, H.; *Mater. Chem. Phys.* **2005**, *90*, 333.

Received: October 8, 2007

Web Release Date: July 23, 2008

FAPESP helped in meeting the publication costs of this article.